

Bayesian Inference and MCMC Methods in Astrophysics

AGASTYA GAUR
University of Illinois at Urbana-Champaign

ABSTRACT

Lorem ipsum dolor sit amet, consectetur adipiscing elit. Etiam lobortis facilisis sem. Nullam nec mi et neque pharetra sollicitudin. Praesent imperdiet mi nec ante. Donec ullamcorper, felis non sodales commodo, lectus velit ultrices augue, a dignissim nibh lectus placerat pede. Vivamus nunc nunc, molestie ut, ultricies vel, semper in, velit. Ut porttitor. Praesent in sapien. Lorem ipsum dolor sit amet, consectetur adipiscing elit. Duis fringilla tristique neque. Sed interdum libero ut metus. Pellentesque placerat. Nam rutrum augue a leo. Morbi sed elit sit amet ante lobortis sollicitudin. Praesent blandit blandit mauris. Praesent lectus tellus, aliquet aliquam, luctus a, egestas a, turpis. Mauris lacinia lorem sit amet ipsum. Nunc quis urna dictum turpis accumsan semper.

Keywords: Astrophysics, Astrostatistics, Bayesian Statistics, Markov Chain Monte Carlo, Big Data

1. INTRODUCTION

1.1. *The History of Astrostatistics*

In the 4th century BC, Hipparchus, attempting to estimate the length of a year, found the middle of the range of a scattered set of Babylonian solstice measurements. An achievement for the time, Hipparchus's measurement marked the beginning of what would become a long-standing marriage between astronomy and statistics. In the centuries to come, a number of breakthroughs in astrostatistics followed. Notably, Tycho Brahe in the late 1500s employed repeated positional measurements of stars and used the mean of the data to map them. His work was so precise that it became the foundation of Kepler's laws of planetary motion, and it took astronomers generations to produce better measurements. (Leavesley & Tárnok 2018). Furthermore, in the 1770s, Laplace rediscovered Bayesian statistics, and over the next decade he continued to expand upon his work, using it in a colossal effort to extend Newton's theory of gravity, work that would have him hailed as a monumental genius (Stigler 1975).

The biggest advancement in astrostatistics before the era of computing came in 1805 when Legendre published the method of least squares regression to model the orbit of comets (Feigelson & Babu 2004). He theorized that the model best fit to a set of data was one that minimized the sum of the squares of the errors. Though Legendre did not provide a formal proof of the method, regarding it only as a convenient trick, later works by Robert Adrain developed formal mathematical proofs of the method (Merriman 1877). In 1809, Gauss published his own work on least squares, showing it

was used to calculate the orbit of the dwarf planet Ceres, even when observing it was impossible due to solar glare. Less elegantly, he also insisted that he had discovered the method years before Legendre (Stigler 1981). As controversial as the development of least squares regression ended up being, it has cemented itself in history as one of the most important leaps in astrostatistics.

The recurring theme was clear: progress in astronomy often hinged on solving problems of statistical estimation. By the end of the century, astronomy had firmly established itself as a quantitative science, driven by the refinement of statistical methods to identify regularities in scattered measurements, fitting orbital models, and quantifying uncertainty in the presence of noise.

1.2. *Resolving the Identity Crisis*

The next 100 years brought two developments that reshaped the relationship between astronomy and statistics: the rise of physics as the foundation of astronomy and the advent of computing, which enabled unprecedented scales of data analysis. As astronomy grew increasingly intertwined with the theories of physics, the field transformed into what we now call astrophysics. As more astronomers began to call themselves astrophysicists, statistics began to fade in prominence. Though a niche field called statistical astronomy persisted, the majority of astronomers made little use of statistics in their work (Feigelson & Babu 2004). The focus shifted to deriving physical models from first principles, and statistical methods were often seen as secondary or even unnecessary. Hubble (1930) determined the fit for the light curve of elliptical galaxies by trial-and-error instead of regression. Zwicky (1937) first observed dark matter using a curve fitted only by eye.

The disdain for statistics stemmed from most astrophysicists' stubborn adherence to Newtonian determinism. Physics was regarded as the fundamental law of nature and an elegant basis for astronomy, while statistics was seen as rough, approximate, and imperfect. Around the same time, statistics flourished in the social sciences, further pushing it from astrophysics.

However, statistics would not be kept away from astronomy for long. As computers developed, astronomers increasingly adopted new tools for both calculation and simulation. In the 1920s, one of the earliest applications appeared in the production of lunar tables. Previously, astronomers calculated the position of the Moon using complex, error-prone methods that required extensive manual computation (Duncombe 1988). By the 1930s, however, Comrie (1932) demonstrated how punch card computing machines could automate the process, making lunar ephemerides faster and more reliable. From then on to the 1970s, Comrie's work was continued by Wallace Eckert, who improved the punch-card calculations using IBM computers (Olley 2018). Like lunar calculations, galactic simulations were also performed with computers as early as the 1940s. Holmberg (1940) modeled gravitational interactions using lightbulbs to represent galaxies, demonstrating how spiral structures could emerge. These analog demonstrations laid the groundwork for fully computational N-body simulations in the 1970s, such as Toomre & Toomre (1972), who used them to explain tidal tails and bridges in interacting galaxies.

With these advances in computing came a natural resurgence of statistical methods in astronomy. The ability to automate calculations, handle larger datasets, and simulate complex systems meant that statistical analysis became not only feasible but indispensable. In the mid-20th century, the growth of galaxy surveys encouraged quantitative treatments of structure and dynamics. Early work such as Lynden-Bell (1967) applied statistical mechanics to stellar systems, laying the foundation for the study of galaxy formation and equilibrium. By the 1970s, statistics was increasingly recognized as

a distinct methodological pillar of astronomy. [Peebles \(1973\)](#) systematically catalogued and analyzed extragalactic objects using power spectra and correlation functions, pioneering the statistical study of large-scale structure.

Where once statistical methods were painfully labor-intensive, computing enabled astronomers to apply them across vast amounts of observational data. While the early history of the field was dominated by statistical reasoning, the growth of physics and computation broadened this into what we now call quantitative analysis (QA). Quantitative analysis thus represents the merging of three traditions that once stood apart: the deductive rigor of physics, the inferential power of statistics, and the scalability of computation. In modern astronomy, progress often relies not on one of these strands in isolation but on their integration. QA therefore serves as both a methodological framework and a philosophy of practice, emphasizing reproducibility, uncertainty quantification, and the ability to extract physical meaning from complex data.

1.3. *The Data Deluge*

Today, astrophysics sits in the middle of a universe of complex statistical problems that demand new quantitative approaches and more computing power with each passing day. In many respects, QA has become the backbone of research in modern astrophysics, and at a pivotal moment as the 21st century has ushered in an unprecedented era of astronomical data generation. Sky surveys like Gaia DR3 alone provide astrometry and photometry for nearly two billion stars, plus more than ten million variable sources across dozens of types ([Gaia Collaboration et al. 2023](#)). The nineteenth data release of the Sloan Digital Sky Survey collected robust spectroscopic data from over 6 million objects ([Collaboration et al. 2025](#)). Advances in CCD detectors will see data from sky surveys continue to grow in the next decade from gigabytes to terabytes today, and possibly to petabytes in the near future. The same trend can be seen in data from NASA’s Solar Dynamics Observatory, which now generates over a terabyte of data per day, and the Rubin LSST, generating close to 30 terabytes per day ([Borne 2009](#)). Compared to the Henry Draper Catalogue ([Cannon & Pickering 1918](#))—a century-old counterpart that cataloged roughly 200,000 stars—the explosion in data is striking.

The leap from hundreds of thousands of stars in the Henry Draper Catalogue to billions in Gaia represents more than a change in scale: it is a qualitative transformation in what science becomes possible. With the Draper Catalogue, astronomers could classify stellar spectra and trace broad patterns in stellar populations. With Gaia, it is now possible to reconstruct the full three-dimensional structure and kinematics of the Milky Way, identify hypervelocity stars, and test theories of Galactic evolution with unprecedented detail. Where older surveys allowed the identification of a few rare stellar types, modern surveys allow systematic searches for extreme outliers across billions of objects, transforming the statistical character of astronomy.

This data deluge makes QA indispensable. Large-scale surveys now span the entire electromagnetic spectrum, from radio (e.g., LOFAR, ALMA) to X-ray and gamma-ray observatories such as Chandra and Fermi. Multi-messenger astronomy adds yet another layer, with gravitational waves detected by LIGO/Virgo and high-energy neutrinos from IceCube ([Abbasi et al. 2023](#)). Time-domain surveys such as ZTF and the upcoming LSST produce streams of transient and variable sources, producing data that are not only high-volume but also high-velocity. This also creates qualitatively harder problems as each modality comes with distinct noise properties, resolutions, and systematic biases, making integration across datasets a formidable statistical task. The ability to extract meaningful insights

from these massive datasets in an organized manner is crucial for advancing our understanding of the universe. QA provides a number of powerful tools spanning statistical inference, computational algorithms, and machine learning methodologies to analyze, interpret, and model this data effectively.

1.4. *Statistical Challenges in Modern Astrophysics*

Across astrophysics, two recurring types of challenges emerge. The first challenge is that noisy, incomplete, and often degenerate data have estimated distributions that differ across multiple competing theories. Though theoretical astrophysics has given us the tools to reduce these problems to estimations of physical constants, the number and complexity of parameters still pose major challenges (Schafer 2015). Such degeneracies manifest across nearly every subfield of astrophysics. For example, in exoplanet studies, radial velocity measurements can only determine a planet’s minimum mass because they can’t reveal whether we are seeing the orbit at an angle. In cosmology, measurements of the cosmic microwave background blur together the effects of the Hubble constant, the amount of ordinary matter, and dark energy, so isolating any one factor requires assumptions about the others. Even within galaxies, rotation curve studies must weigh the balance between visible stars and invisible dark matter. Each of these cases requires careful statistical treatment to avoid misleading conclusions.

The second challenge is that the large volume of data creates equally daunting problems of computing time and power. The Rubin Observatory LSST will generate tens of terabytes of imaging data per night (Borne 2009), while Gaia has already released petabyte-scale catalogs (Gaia Collaboration et al. 2023). Brute-force exploration of parameter spaces is simply impossible at these scales. Efficient algorithms and scalable statistical methods are required to render analysis computationally tractable (Huijse et al. 2014). Without such methods, the majority of information encoded in these massive datasets would remain inaccessible. Together, these issues create a need for QA frameworks that can both handle degeneracy in complex parameter spaces and scale efficiently with massive datasets.

1.5. *Bayesian Inference and MCMC in Context*

Within this landscape, Bayesian inference via Markov Chain Monte Carlo (MCMC) methods naturally emerges as a potential solution.. Bayesian inference offers a principled framework for parameter estimation in complex systems, and MCMC methods provide an effective way to explore parameter spaces by sampling from posterior distributions. For astrophysicists, this has become one of the most widely used and versatile approaches. Von Toussaint (2011) notes the growing applicability of Bayesian inference in physics. Computational models are becoming far more complex, and the data being analyzed is often noisy and incomplete. Bayesian methods, with their ability to incorporate prior knowledge and handle uncertainty, are particularly well-suited to these challenges. MCMC methods, in particular, provide a practical way to sample from complex posterior distributions that arise in Bayesian analysis. This makes them invaluable for parameter estimation, model comparison, and uncertainty quantification in almost any astrophysical problem.

Another reason for the appeal of Bayesian methods is their contrast with frequentist approaches. Frequentist methods, which were dominant through much of the 20th century, emphasize point estimates and confidence intervals derived from repeated sampling arguments. Bayesian inference, in contrast, provides full posterior probability distributions for parameters, naturally incorporating

prior information from physics or earlier observations. This framework is particularly powerful in astrophysics, where data are sparse, noisy, and often incomplete.

The systematic adoption of Bayesian statistics in astronomy gained momentum in the late 20th century. Cosmologists applied Bayesian methods to the cosmic microwave background; for example, works by Tegmark et al. (1997) and others showing how to extract cosmological parameters from noisy sky maps. In exoplanet science, Bayesian inference became standard in the 1990s and 2000s for modeling radial velocity curves and transit signals, which proved successful as datasets grew larger and more precise (Gregory 2005). Pulsar timing, supernova cosmology, and gravitational lens modeling similarly saw Bayesian methods supplanted heuristic or purely frequentist treatments. The trend reflects a broader recognition that many of astronomy’s hardest problems demand not just point estimates, but principled uncertainty quantification.

This review adopts a QA perspective and centers on Bayesian inference and MCMC because of their flexibility, principled uncertainty quantification, and growing ubiquity across astrophysics. In Section II, the methodology section develops a working foundation: it reviews Bayesian statistics, motivates priors and likelihood construction in realistic astronomical settings, and walks through toy examples before escalating to domain-relevant formulations; it then introduces Monte Carlo methods and builds to Markov Chain Monte Carlo, deriving the Metropolis family and related samplers, and provides step-by-step Python implementations on simple problems.

Section III presents three focused case studies that illustrate how Bayesian–MCMC pipelines advance frontiers in different subfields while confronting distinct sources of noise, degeneracy, and computational load. For exoplanet direct detection, the section sketches the observational context and the central challenge of disentangling planetary signals from stellar activity and disk structure; it then outlines joint stellar–planet modeling with Gaussian processes and Bayesian classification frameworks for robust detections and non-detections, highlighting benefits and failure modes in low SNR regimes. For CMB parameter estimation, it explains geometric degeneracies in the power spectrum and shows how MCMC accelerators and parallelizable frameworks enable efficient exploration and evidence calculations, including tradeoffs between sampler sophistication and wall-clock efficiency. For gravitational-wave inference, it frames waveform fitting in high-dimensional parameter spaces, discusses the cost of likelihood evaluations, and motivates gradient-informed MCMC strategies that reduce computation without compromising accuracy, with notes on priors, calibration systematics, and real-time constraints.

Finally, Section IV and V compare cases where Bayesian–MCMC excels with those where complementary methods are more appropriate, identify methodological gaps revealed by the case studies (e.g., scalable likelihoods, robust priors, multimodal posterior handling), and outline opportunities for future work in astrophysics and related fields that face similar statistical and computational challenges.

2. METHODOLOGY

2.1. Foundations of Bayesian Statistics

The aim of Bayesian statistics is simple: determine $P(H|D)$, or the probability of a hypotheses H being true given data D . A hypothesis is any statement that can be true or false, and data is any information that can be used to evaluate the hypothesis. For example, imagine rolling a die. A hypothesis H would that the die roll is a 3. The data D is the result of the die roll.

Hypotheses live in the *hypothesis space*, which is the set of all possible hypotheses of a system (Brewer 2018). Going back to the die example, the hypothesis space is $\{1, 2, 3, 4, 5, 6\}$. The hypothesis space will also have a probability distribution, or a *prior*, written as $P(H)$. The prior is the probability of each hypothesis being true before seeing any data. For a fair die, the prior is uniform. It's $\frac{1}{6}$ for all H in the hypothesis space. In other words, $P(H)$ is the probability of the hypothesis being true.

The data D also has a probability distribution called the *evidence*, $P(D)$ (Brewer 2018). The evidence is the probability of seeing the data before knowing anything about the hypothesis. In the die example, if you roll a 3, then $P(D)$ is $\frac{1}{6}$ because there is a $\frac{1}{6}$ chance of rolling a 3 on a fair die. The evidence lives in the *data space*, which is the set of all possible data of a system. In the die example, the data space is also $\{1, 2, 3, 4, 5, 6\}$.

A *likelihood*, $P(D|H)$, is the probability of seeing the data assuming that the hypothesis is true. In the die example, if H is that the die roll is a 3, then $P(D|H)$ is 1 if the die roll is a 3 and 0 otherwise. Using the prior, evidence, and likelihood to calculate $P(H|D)$, which is the probability of a hypothesis being true given the data. This is called the *posterior*. In the die example, if you roll a 3, then $P(H|D)$ is 1 if H is that the die roll is a 3 and 0 otherwise.

The framework for finding $P(H|D)$ is called Bayes' Theorem, and it forms the center of Bayesian inference. It can be derived using two rules (Cox 1946). Firstly, the probability that a hypothesis is true and the probability that it is not true add up to 1:

$$P(H) + P(\tilde{H}) = 1. \quad (2.1)$$

The second rule is the product rule, which states:

$$P(H)P(D|H) = P(D)P(H|D). \quad (2.2)$$

This can be trivially rearranged to give Bayes' Theorem:

$$P(H|D) = \frac{P(H)P(D|H)}{P(D)}. \quad (2.3)$$

In other words, given the prior, evidence, and the likelihood, you can calculate the posterior $P(H|D)$.

2.1.1. Example: The Double-Headed Coin

The previous example of a die roll was trivial. The data, the result of the die roll, completely determined the hypothesis. Bayesian statistics becomes more useful when the data is incomplete, as is often the case in Astrophysics.

To demonstrate this, consider the following setup. You have 5 coins, four of which are fair, and one of which is double-headed. You pick a coin at random and flip it, and it lands heads. *What is the probability that you picked the double-headed coin?*

The first step is to determine H and D from the hypotheses and data spaces. The hypothesis space is $\{\text{Picked Fair}, \text{Picked Double-Headed}\}$. For the sake of conciseness, it can be written as $\{\text{fair}, \text{double}\}$. For this problem, we hypothesize that the double-headed coin was picked. So, H is 'double'. The data space is $\{\text{heads}, \text{tails}\}$, and for this problem, D is 'heads'.

Next, we determine the prior and evidence. There are 4 fair coins and 1 double-headed coin, so it is easy to find for the prior that $P(\text{fair}) = \frac{4}{5} = 0.8$ and $P(\text{double}) = \frac{1}{5} = 0.2$. The evidence is more complex to find in this case. Since the chance of flipping heads or tails includes the case that you picked up the double headed coin, the evidence cannot simply be 50-50. We must calculate the mean probability of getting heads and tails across all the coins:

$$\begin{aligned} P(\text{heads}) &= \frac{0.5 + 0.5 + 0.5 + 0.5 + 1}{5} = 0.6 \\ P(\text{tails}) &= \frac{0.5 + 0.5 + 0.5 + 0.5}{5} = 0.4 \end{aligned}$$

Note the implicit rule for any space:

$$\sum_n P(x_n) = 1, \quad (2.4)$$

where x_n is a value in a space.

The final step before solving is to find the likelihood, $P(\text{heads}|\text{double})$. This is trivially 1, as you can only get heads from the double-headed coin. Now, we can solve for the posterior:

$$P(\text{double}|\text{heads}) = \frac{P(\text{double})P(\text{heads}|\text{double})}{P(\text{heads})} = \frac{0.2}{0.6} = \boxed{0.\bar{3}}$$

Before incorporating the data, the probability of picking the double headed coin was 0.2, but by using Bayesian statistics, we were able to "learn" from the data and increase the probability to $0.\bar{3}$. This is a simple example, but it demonstrates the power of Bayesian statistics in the face of incomplete data.

2.2. Bayesian Statistics in Astrophysics

In an astrophysical context, Bayes' Theorem is used to calculate the probability of *parameters*, θ , of a model rather than a hypothesis ([Brewer 2018](#)).

$$P(\theta|D) = \frac{P(\theta)P(D|\theta)}{P(D)}. \quad (2.5)$$

Take, for example, measurements of the radial velocity of a star over time. When a star hosts an orbiting planet, both bodies orbit a common center of mass. This induces a 'wobble' in the star's motion which is detected as periodic Doppler shifts from the star's spectrum, also known as the *radial velocity*. The radial velocity $v_r(t)$ of a star with a single planet can be modeled as:

$$v_r(t) = K \sin\left(\frac{2\pi t}{T} + \phi\right), \quad (2.6)$$

where K is the velocity semi-amplitude, T is the orbital period, and ϕ is a phase offset. Thus, the parameters of this model are $\theta = \{K, P, \phi\}$.

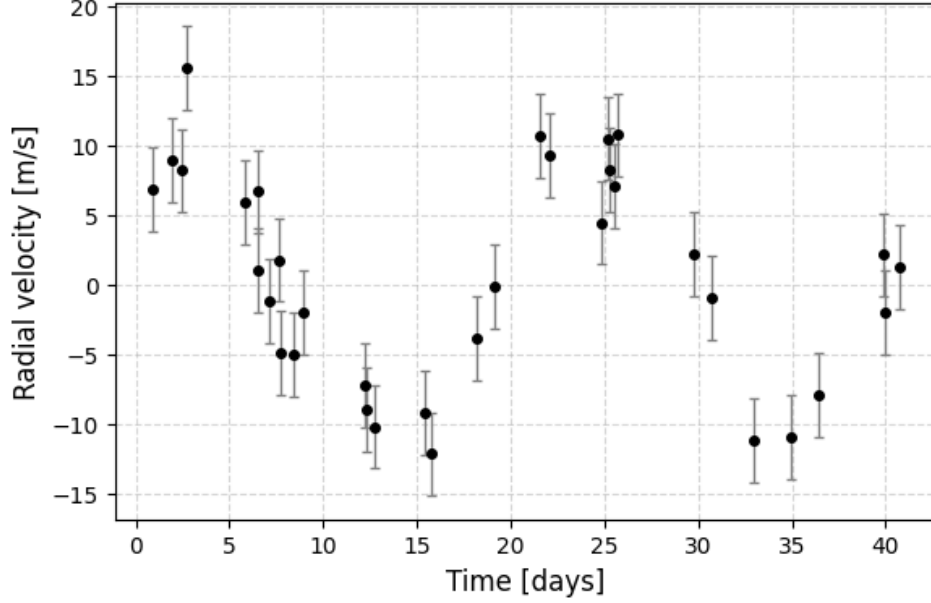


Figure 1. Simulated radial velocity data of a star with a single orbiting planet. Each point has an error of three standard deviations. The data is noisy and incomplete, making it difficult to determine the parameters of the model.

One could measure the radial velocity of a star over a certain time period and obtain the data shown in [Figure 1](#).

Bayes' Theorem can be used to determine the posterior distribution of the parameters using the noisy, incomplete data. In this case, [Equation 2.3](#) becomes:

$$P(K, T, \phi | D) = \frac{P(K, T, \phi) P(D | K, T, \phi)}{P(D)}. \quad (2.7)$$

To start, we must determine the prior, $P(K, T, \phi)$. For simplicity, we can assume that the parameters are independent, so the prior can be written as:

$$P(K, T, \phi) = P(K)P(T)P(\phi). \quad (2.8)$$

Since we know nothing about the priors, it is reasonable to assume that they are uniformly distributed in a certain range. Looking at the data, we can see that the velocity semi-amplitude K is between 5 and 15 m/s, the period T is between 20 and 30 days, and the phase offset ϕ is between 0 and 2π . Thus, the priors are:

$$P(K) = \begin{cases} \frac{1}{10} & 5 < K < 15 \\ 0 & \text{otherwise} \end{cases} \quad P(T) = \begin{cases} \frac{1}{10} & 20 < T < 30 \\ 0 & \text{otherwise} \end{cases} \quad P(\phi) = \begin{cases} \frac{1}{2\pi} & 0 < \phi < 2\pi \\ 0 & \text{otherwise} \end{cases}$$

and the combined prior is then:

$$P(K, T, \phi) = \begin{cases} \frac{1}{200\pi} & 5 < K < 15, 20 < T < 30, 0 < \phi < 2\pi \\ 0 & \text{otherwise} \end{cases} \quad (2.9)$$

Next, we must determine the likelihood, $P(D|K, T, \phi)$, or the probability of seeing the data given the parameters. To do this, we calculate the probability of seeing each data point given what the model would predict for that data point. We can assume the model prediction is the mean of a normal distribution of possible points, and the error of each data point is the standard deviation. Using this, we can calculate the probability of obtaining a data point d_i at time t_i . Multiplying the probabilities of all the data points gives the probability of seeing the full dataset, which is the likelihood. Mathematically, this is:

$$P(D|K, T, \phi) = \prod_{i=1}^N \frac{1}{\sqrt{2\pi\sigma_i^2}} \exp\left(-\frac{(D_i - v_r(t_i; K, T, \phi))^2}{2\sigma_i^2}\right), \quad (2.10)$$

Substituting values for each parameter gives the likelihood of seeing the data given the parameters.

Finally, we must determine the evidence, $P(D)$. It's obvious that when integrating the posterior over the entire parameter space, it must equal one, as the parameters are certain to take on some value within the space. Thus, the evidence can be found by rearranging the equation:

$$\begin{aligned} 1 &= \iiint P(K, T, \phi|D) dK dT d\phi \\ 1 &= \iiint \frac{P(K, T, \phi)P(D|K, T, \phi)}{P(D)} dK dT d\phi \\ \therefore P(D) &= \iiint P(K, T, \phi)P(D|K, T, \phi) dK dT d\phi \end{aligned} \quad (2.11)$$

Note that this integral is analytically intractable, so it must be calculated numerically.

Using the data in [Figure 1](#), we can calculate the posterior distribution of the parameters using the code given in [Appendix A](#). The results are shown in [Figure 2](#).

In reality, we will never know the exact parameters of a system, but posterior distributions give us a close estimate. To quantify how close the estimate is, we will compare the posterior distributions to the true parameters, which are $K = 10$ m/s, $T = 25$ days, and $\phi = \frac{\pi}{4}$. It is clear to see that the true values are within one standard deviation of the mean of each posterior distribution, indicating that the Bayesian method was successful in estimating the parameters.

[Figure 3](#) shows the true model along with the mean prediction from the posterior distributions. Thus, we can apply Bayes' Theorem to predict the parameters for astrophysical models. However, this method is computationally expensive. Computing this numerically, we would have to iterate through all combinations of all values of each parameter. With n parameters and m possible values for each parameter, this algorithm would have a time complexity of $O(m^n)$, which is infeasible for even small n and m . To solve this problem, we can use *Monte Carlo methods*.

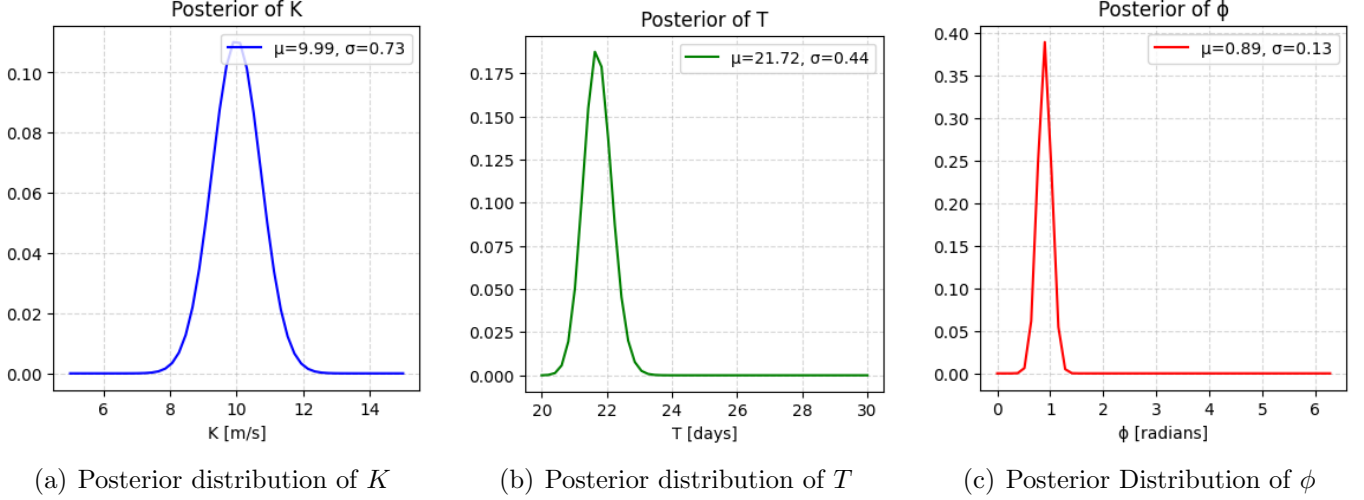


Figure 2. The marginal posterior distributions of the parameters K , T , and ϕ given the data in Figure 1. These posteriors are normalized with a numerically calculated evidence.

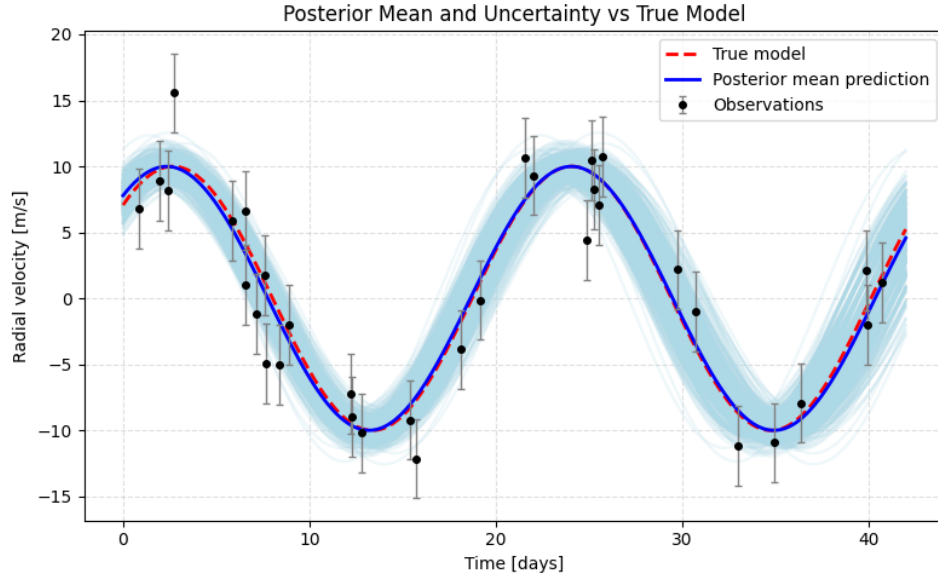


Figure 3. The radial velocity data from Figure 1 along with the mean prediction from the posterior distributions in Figure 2. The shaded region represents one standard deviation from the mean prediction.

2.3. Monte Carlo Sampling

The primary computational challenge in brute force Bayesian inference arises from evaluating the posterior probability at every point in the parameter space. One way to reduce this cost is to sample only a subset of points, distributed according to the posterior itself. These points are called *draws*. If, by some method, a set of draws were obtained, it would be possible to calculate expectation values from the explicit posterior using only the sampled points (Von Toussaint 2011). This is the idea behind *Monte Carlo Sampling*, which can be used to approximate integrals and expectations that would otherwise require explicit evaluation over a continuous space.

x	Description
θ_i	Expectation value of parameter θ_i
θ_i^2	Variance of parameter θ_i
$f(\theta_1, \theta_2, \dots, \theta_n)$	Expectation value of any function of the parameters
$\mathbb{1}(\theta_i = a)$	Probability that $\theta_i = a$
$\mathbb{1}(a \leq \theta_i \leq b)$	Probability that θ_i is in the range $[a, b]$
$\mathbb{1}(\text{condition})$	Probability that the condition is true

Table 1. Forms of x to calculate expectation values of different quantities.

If we know a probability density explicitly, the expectation value of some variable x can be calculated as:

$$\langle x \rangle = \int x P(\theta) dx. \quad (2.12)$$

Using a set of N values of x drawn using Monte Carlo, this can be approximated as:

$$\langle x \rangle \approx \frac{1}{N} \sum_{i=1}^N x_i, \quad (2.13)$$

which generalizes naturally to higher-dimensional parameter spaces, though convergence can become slower as dimensionality increases.

x is a function of the parameters, and can be defined arbitrarily to calculate the expectation value of any value of interest. Given a probability density $P(\theta_1, \theta_2, \dots, \theta_n)$, some forms of x are listed in [Table 1](#).

The usefulness of Monte Carlo sampling becomes apparent when we revisit the computation of marginal posteriors. In the previous example, we used the posterior to calculate the marginal posteriors of each parameter. In the brute force method, this was found by integrating the posterior over all other parameters. Monte Carlo makes this simpler. If we have a set of N draws from the posterior of a parameter space with parameters, $\{\theta_1, \theta_2, \dots, \theta_n\}$, we can obtain draws for a certain parameter θ_i by simply ignoring all other parameters. Information about the marginal posterior can then be calculated from those draws as needed.

2.4. Markov Chain Monte Carlo

Before we can use Monte Carlo sampling, we must first obtain draws from the posterior. *Markov Chain Monte Carlo* is one of the many methods used to obtain these draws, and in modern astrophysics, has become a standard tool for Bayesian inference.

2.4.1. Markov Chains

A *Markov Chain* is a sequence of random variables, X_1, X_2, \dots, X_n , where the probability of each variable only depends on the previous variable ([Trotta 2008](#)). This is known as the *Markov Property*, and can be written mathematically as:

$$P(X_n|X_{n-1}, X_{n-2}, \dots, X_1) = P(X_n|X_{n-1}). \quad (2.14)$$

2.5. Implementations

2.5.1. Software Ecosystem

2.5.2. Common Challenges in Astrophysics

APPENDIX

A. RADIAL VELOCITY SOURCE CODE

```

1  ###
2  # --- Radial Velocity Example ---
3  # This script demonstrates simple Bayesian parameter estimation for a
4  # sinusoidal radial velocity model of the form:
5  # v(t) = K * sin(2 * pi * t / P + phi)
6
7  import numpy as np
8  import matplotlib.pyplot as plt
9
10 np.random.seed(42) # The meaning of life for reproducibility
11
12 ###
13 # --- True Parameter Values ---
14 K = 10.0 # Velocity semi-amplitude [m/s]
15 P = 21.4 # Period of the signal [days]
16 phi = 0.25 * np.pi # Phase offset [radians]
17 sig_ob = 3.0 # Observational uncertainty [m/s]
18
19 ###
20 # --- Generate Synthetic Data ---
21 # Simulate 34 observations across 42 days
22 t = np.sort(42 * np.random.rand(34))
23
24 # Observed velocities = true model + Gaussian noise
25 v_ob = K * np.sin((2 * np.pi * t / P) + phi) + np.random.normal(0, sig_ob,
26     size=len(t))
27
28 ###
29 # --- Plot Observations Only ---
30 plt.figure(figsize=(6, 4))
31 plt.errorbar(
32     t, v_ob, yerr=sig_ob, fmt='o', color='black',
33     ecolor='gray', elinewidth=1, capsize=2,
34     label='Observations', markersize=4
35 )

```

```

35 plt.xlabel("Time [days]", fontsize=12)
36 plt.ylabel("Radial velocity [m/s]", fontsize=12)
37 plt.grid(True, linestyle='--', alpha=0.5)
38 plt.tight_layout()
39 plt.show()
40
41 ###
42 # --- Plot Observations and True Model ---
43 t_dense = np.linspace(0, 42, 1000)
44 plt.figure(figsize=(6, 4))
45 plt.errorbar(
46     t, v_ob, yerr=sig_ob, fmt='o', color='black',
47     ecolor='gray', elinewidth=1, capsize=2,
48     label='Observations', markersize=4
49 )
50 plt.plot(t_dense, K * np.sin(2 * np.pi * (t_dense / P) + phi),
51          'r--', linewidth=2, label='True model')
52 plt.xlabel("Time [days]", fontsize=12)
53 plt.ylabel("Radial velocity [m/s]", fontsize=12)
54 plt.grid(True, linestyle='--', alpha=0.5)
55 plt.tight_layout()
56 plt.show()
57
58 ###
59 # --- Brute-Force Bayesian Parameter Estimation ---
60 # Define prior, likelihood, and posterior functions
61
62 # Uniform prior over plausible parameter ranges
63 def prior(K, P, phi):
64     if 5 < K < 15 and 20 < P < 30 and 0 < phi < 2 * np.pi:
65         return 1 / (10 * 10 * 2 * np.pi)
66     else:
67         return 0
68
69 # Gaussian likelihood assuming constant sigma
70 def likelihood(K, P, phi, t, v_ob, sig_ob):
71     v_model = K * np.sin((2 * np.pi * t / P) + phi)
72     return np.prod(
73         (1 / (np.sqrt(2 * np.pi) * sig_ob)) *
74         np.exp(-((v_ob - v_model) ** 2) / (2 * sig_ob ** 2))
75     )
76
77 # Posterior = prior * likelihood
78 def posterior(K, P, phi, t, v_ob, sig_ob):
79     return likelihood(K, P, phi, t, v_ob, sig_ob) * prior(K, P, phi)
80
81 ###
82 # --- Evaluate Posterior on a Grid ---

```

```

83 K_vals = np.linspace(5, 15, 50)
84 P_vals = np.linspace(20, 30, 50)
85 phi_vals = np.linspace(0, 2 * np.pi, 50)
86 posterior_vals = np.zeros((len(K_vals), len(P_vals), len(phi_vals)))
87
88 norm = 0
89 for i, K_i in enumerate(K_vals):
90     for j, P_j in enumerate(P_vals):
91         for k, phi_k in enumerate(phi_vals):
92             posterior_vals[i, j, k] = posterior(K_i, P_j, phi_k, t, v_ob,
93                 sig_ob)
94             norm += posterior_vals[i, j, k]
95 posterior_vals /= norm
96
97 ###
98 # --- Compute Marginal Posteriors and Statistics ---
99 posterior_K = np.sum(np.sum(posterior_vals, axis=2), axis=1)
100 posterior_P = np.sum(np.sum(posterior_vals, axis=0), axis=1)
101 posterior_phi = np.sum(np.sum(posterior_vals, axis=0), axis=0)
102
103 mean_K = np.sum(K_vals * posterior_K) / np.sum(posterior_K)
104 std_K = np.sqrt(np.sum((K_vals - mean_K) ** 2 * posterior_K) / np.sum(
105     posterior_K))
106 mean_P = np.sum(P_vals * posterior_P) / np.sum(posterior_P)
107 std_P = np.sqrt(np.sum((P_vals - mean_P) ** 2 * posterior_P) / np.sum(
108     posterior_P))
109 mean_phi = np.sum(phi_vals * posterior_phi) / np.sum(posterior_phi)
110 std_phi = np.sqrt(np.sum((phi_vals - mean_phi) ** 2 * posterior_phi) / np
111     .sum(posterior_phi))
112
113 ###
114 # --- Plot Marginal Posterior Distributions ---
115 plt.figure(figsize=(4, 4))
116 plt.plot(K_vals, posterior_K, color='blue', label=f"mu={mean_K:.2f}, sigma
117     ={std_K:.2f}")
118 plt.xlabel("K [m/s]")
119 plt.title("Posterior of K")
120 plt.legend()
121 plt.grid(True, linestyle='--', alpha=0.5)
122 plt.show()
123
124 plt.figure(figsize=(4, 4))
125 plt.plot(P_vals, posterior_P, color='green', label=f"mu={mean_P:.2f},
126     sigma={std_P:.2f}")
127 plt.xlabel("P [days]")
128 plt.title("Posterior of P")
129 plt.legend()
130 plt.grid(True, linestyle='--', alpha=0.5)

```



```

125 plt.show()
126
127 plt.figure(figsize=(4, 4))
128 plt.plot(phi_vals, posterior_phi, color='red', label=f"mu={mean_phi:.2f},
129          sigma={std_phi:.2f}")
129 plt.xlabel("phi [radians]")
130 plt.title("Posterior of phi")
131 plt.legend()
132 plt.grid(True, linestyle='--', alpha=0.5)
133 plt.show()
134
135 ###
136 # --- Compare True Model vs Posterior Predictions ---
137 plt.figure(figsize=(8, 5))
138 N_samples = 500
139
140 for i in range(N_samples):
141     K_draw = np.random.choice(K_vals, p=posterior_K)
142     P_draw = np.random.choice(P_vals, p=posterior_P)
143     phi_draw = np.random.choice(phi_vals, p=posterior_phi)
144     plt.plot(t_dense, K_draw * np.sin(2 * np.pi * (t_dense / P_draw) +
145          phi_draw),
146             color='lightblue', alpha=0.2)
147
148 plt.plot(t_dense, K * np.sin(2 * np.pi * (t_dense / P) + phi),
149          'r--', lw=2, label='True model')
150 plt.plot(t_dense, mean_K * np.sin(2 * np.pi * (t_dense / mean_P) +
151          mean_phi),
152          'b--', lw=2, label='Posterior mean prediction')
153
154 plt.errorbar(t, v_ob, yerr=sig_ob, fmt='o', color='black',
155             ecolord='gray', elinewidth=1, capsize=2,
156             label='Observations', markersize=4)
157 plt.xlabel("Time [days]")
158 plt.ylabel("Radial velocity [m/s]")
159 plt.title("Posterior Mean and Uncertainty vs True Model")
160 plt.legend()
161 plt.grid(True, linestyle='--', alpha=0.4)
162 plt.tight_layout()
163 plt.show()
164 # %%

```

REFERENCES

- | | |
|--|--|
| <p>Abbasi, R., Ackermann, M., Adams, J., et al.
 2023, The Astrophysical Journal, 959, 96,
 doi: 10.3847/1538-4357/aceefc</p> | <p>Borne, K. D. 2009, Astrominformatics: A 21st
 Century Approach to Astronomy, arXiv,
 doi: 10.48550/arXiv.0909.3892</p> |
|--|--|

- Brewer, B. J. 2018, in *Bayesian Astrophysics*, ed. A. A. Ramos & I. Arregui (Cambridge: Cambridge university press)
- Cannon, A. J., & Pickering, E. C. 1918, *The Henry Draper Catalogue* (The Observatory)
- Collaboration, SDSS., Pallathadka, G. A., Aghakhanloo, M., et al. 2025, *The Nineteenth Data Release of the Sloan Digital Sky Survey*, arXiv, doi: [10.48550/arXiv.2507.07093](https://doi.org/10.48550/arXiv.2507.07093)
- Comrie, L. J. 1932, *Monthly Notices of the Royal Astronomical Society*, 92, 694, doi: [10.1093/mnras/92.7.694](https://doi.org/10.1093/mnras/92.7.694)
- Cox, R. T. 1946, *American Journal of Physics*, 14, 1, doi: [10.1119/1.1990764](https://doi.org/10.1119/1.1990764)
- Duncombe, R. L. 1988, *Celestial Mechanics*, 45, 1, doi: [10.1007/BF01228969](https://doi.org/10.1007/BF01228969)
- Feigelson, E. D., & Babu, G. J. 2004, *Statistical Challenges in Modern Astronomy*, arXiv, doi: [10.48550/arXiv.astro-ph/0401404](https://doi.org/10.48550/arXiv.astro-ph/0401404)
- Gaia Collaboration, Vallenari, A., Brown, A. G. A., et al. 2023, *Astronomy & Astrophysics*, 674, A1, doi: [10.1051/0004-6361/202243940](https://doi.org/10.1051/0004-6361/202243940)
- Gregory, P. C. 2005, *The Astrophysical Journal*, 631, 1198, doi: [10.1086/432594](https://doi.org/10.1086/432594)
- Holmberg, E. 1940, *The Astrophysical Journal*, 92, 200, doi: [10.1086/144212](https://doi.org/10.1086/144212)
- Hubble, E. P. 1930, *The Astrophysical Journal*, 71, 231, doi: [10.1086/143250](https://doi.org/10.1086/143250)
- Huijse, P., Estevez, P. A., Protopapas, P., Principe, J. C., & Zegers, P. 2014, *IEEE Computational Intelligence Magazine*, 9, 27, doi: [10.1109/MCI.2014.2326100](https://doi.org/10.1109/MCI.2014.2326100)
- Leavesley, S., & Tárnok, A. 2018, *Cytometry Part A*, 93, 977, doi: [10.1002/cyto.a.23637](https://doi.org/10.1002/cyto.a.23637)
- Lynden-Bell, D. 1967, *Monthly Notices of the Royal Astronomical Society*, 136, 101, doi: [10.1093/mnras/136.1.101](https://doi.org/10.1093/mnras/136.1.101)
- Merriman, M. 1877, *The Analyst*, 4, 33, doi: [10.2307/2635472](https://doi.org/10.2307/2635472)
- Olley, A. 2018, *Revue de Synthèse*, 139, 267, doi: [10.1163/19552343-13900014](https://doi.org/10.1163/19552343-13900014)
- Peebles, P. J. E. 1973, *The Astrophysical Journal*, 185, 413, doi: [10.1086/152431](https://doi.org/10.1086/152431)
- Schafer, C. M. 2015, *Annual Review of Statistics and Its Application*, 2, 141, doi: [10.1146/annurev-statistics-022513-115538](https://doi.org/10.1146/annurev-statistics-022513-115538)
- Stigler, S. M. 1975, *Biometrika*, 62, 503, doi: [10.1093/biomet/62.2.503](https://doi.org/10.1093/biomet/62.2.503)
- . 1981, *The Annals of Statistics*, 9, 465
- Tegmark, M., Taylor, A., & Heavens, A. 1997, *The Astrophysical Journal*, 480, 22, doi: [10.1086/303939](https://doi.org/10.1086/303939)
- Toomre, A., & Toomre, J. 1972, *The Astrophysical Journal*, 178, 623, doi: [10.1086/151823](https://doi.org/10.1086/151823)
- Trotta, R. 2008, *Contemporary Physics*, 49, 71, doi: [10.1080/00107510802066753](https://doi.org/10.1080/00107510802066753)
- Von Toussaint, U. 2011, *Reviews of Modern Physics*, 83, 943, doi: [10.1103/RevModPhys.83.943](https://doi.org/10.1103/RevModPhys.83.943)
- Zwicky, F. 1937, *The Astrophysical Journal*, 86, 217, doi: [10.1086/143864](https://doi.org/10.1086/143864)